

# Quantum Billiards in Optical Lattices

Simone Montangero,<sup>1</sup> Diego Frustaglia,<sup>2</sup> Tommaso Calarco,<sup>3</sup> and Rosario Fazio<sup>1,4</sup>

<sup>1</sup>*NEST-CNR-INFM & Scuola Normale Superiore, Piazza dei Cavalieri 7, I-56126 Pisa, Italy*

<sup>2</sup>*Departamento de Física Aplicada II, Universidad de Sevilla, E-41012 Sevilla, Spain*

<sup>3</sup>*Institute for Quantum Information Processing, University of Ulm, D-89069 Ulm, Germany*

<sup>4</sup>*International School for Advanced Studies (SISSA), via Beirut 2-4, I-34014 Trieste, Italy*

We study finite two dimensional spin lattices with definite geometry (spin billiards) demonstrating the display of collective integrable or chaotic dynamics depending on their shape. We show that such systems can be quantum simulated by ultra-cold atoms in optical lattices and discuss how to identify their dynamical features in a realistic experimental setup. Possible applications are the simulation of quantum information tasks in mesoscopic devices.

During the last decades, billiards have been the testbed of classical and quantum chaos [1, 2] due to their simplicity united to the richness of their displayed dynamics [3]. Theoretical evidences of the quantum manifestation of chaos in billiards were first confirmed experimentally in the spectral statistic of microwave resonators [4], quasi-two-dimensional superconducting resonators [5], and atom-optic billiards [6]. A very important step forward in the field occurred when it was realized that the properties of mesoscopic systems could be very sensitive, under appropriate circumstances, to the integrability properties of the underlying classical model [7]. We recall, as an example, the study of conductance fluctuations in quantum dots [8]. More generally, quantum billiards have shown to determine the dynamical properties of charge [9], spin [10] and entanglement [11] in nanostructures. The physics associated to quantum billiards has been shown very recently to be relevant in the study of graphene [12].

The ongoing interest in the study of quantum chaos stimulates the search for new physical systems where it is possible to experimentally study complex dynamical behaviour. In this Letter we propose to realize quantum billiards using optical lattices, which have been proved to be an excellent arena to study quantum many-body systems [13].

Fundamental to our proposal is that optical lattices can operate as universal simulators [14], i.e., by means of an appropriate dynamical control it is possible to reproduce the dynamics of any given spin Hamiltonian. Moreover, by means of the modelling of the form of the external trap it is possible to effectively define finite-size lattices. The class of billiards defined in this work are finite two dimensional optical lattices of given geometry, where collective excitations propagate and interfere as they back-reflect against the geometrical boundaries of the lattice. We therefore talk about *spin billiards*. This class shows a rich set of possible configurations, serving as a model system for different implementations: Depending on the system size, boundary conditions, lattice coordination number, and interaction Hamiltonian between the spins, one can either recover the known results on quantum billiards or

model new physical systems showing original features. In the realm of cold atomic gases the distinction between regular and chaotic dynamics will appear in the momentum distribution of the atoms or in the fluorescence signal. Present-day technology permits the simulation of the spin billiards introduced here.

Optical lattices offer unique possibilities to simulate chaotic or integrable dynamics in a controlled way. The possibility to study billiards in this context gives a brand new perspective to a classic, and well studied, problem; numerous new questions can be addressed. On one side it is possible to explore the transition to chaos in a number of different spin-Hamiltonian depending of its symmetries. On the other side it is essential to understand the realization of the billiard, the measurement of relevant quantities and the sources of imperfections that may mask the physics we want to describe. We decide to first address this last topics. To this end we consider a model Hamiltonian which can be mapped on that of a particle hopping on a finite lattice (the billiard). We will use the language of spin as it is natural in this case and it applies also to those Hamiltonians where the mapping to a tight-binding model does not apply.

*The model* - We consider a two dimensional 1/2-spin lattice with nearest-neighbor  $XX$  interaction in a transverse magnetic field. The Hamiltonian reads

$$\mathcal{H} = \lambda \sum_{\langle m, m' \rangle} (\sigma_x^m \sigma_x^{m'} + \sigma_y^m \sigma_y^{m'}) + \sum_m \sigma_z^m \quad (1)$$

where  $\sigma_\alpha^i$  are the Pauli matrices,  $m = \mathcal{M}(i, j)$  is the composed index of the two dimensional qubits coding  $\{i, j\}$ , and the sum  $\langle m, m' \rangle$  runs over nearest-neighbor spins on a square lattice with coordination number four (except at the boundaries) and free boundary conditions. We set  $\lambda = 1$  and  $\hbar = 1$ . As  $\mathcal{H}$  commutes with the total magnetization, we restrict to the subspace with total magnetization equal to one (in this particular sector a mapping onto the single particle problem applies). The discrete space structure is a key-feature of optical lattices, we therefore need to re-discuss the effect of different billiard shapes on the dynamics. The first billiard under consideration is rectangular (billiard R, Fig. 1, left). We

simulate the time evolution of a wave function initially peaked in an angle (single spin flipped, see Fig. 1 A). This situation can be realized by starting from a Mott insulator state with unit occupancy in a two-dimensional optical lattice [15]. Two atomic hyperfine levels serve as the two pseudo-spin states, and all atoms can be prepared in one of the two by optical pumping. A laser can then be used to excite atoms from specific lattice sites to untrapped (continuum) states, removing them from the lattice. Its focus can be swept all along the border of a pre-defined region, leaving a regularly filled lattice of uniformly polarized atoms corresponding to the chosen billiard shape. At this point a Raman  $\pi$ -pulse on resonance with the transition between the two hyperfine levels can be used to flip the state of one atom at one of the billiard's vertices. In this particular geometry, shining the vertex atom with the edge of the laser spot will suffice, eliminating the need for subwavelength addressing. The simulation of the propagation of the resulting spin wave can then take place following a stroboscopic procedure based on lattice-driven state-dependent collisions between neighboring atoms [14, 16]. Billiard S (Fig. 1, right) is a quarter of a Bunimovich stadium and the initial condition is, as before, localized at a boundary angle (see Fig. 1 B). In both cases, the initial condition reads

$$|\psi_{t=0}\rangle \equiv |\mathcal{M}(0, 0)\rangle. \quad (2)$$

Note that our analysis applies also to four-fold symmetric billiards, the symmetry axis of which passes through the site of the initial excitation  $\mathcal{M}(0, 0)$ . Our choice allows us to study the time evolution of an excitation neglecting the effects of central and axial symmetries. The initial condition (2) is such that the dynamics will be influenced also by very high energy levels, i.e., the dynamics is very far from being composed only by the low-lying excitations. On the contrary, in the continuum limit and starting with a different initial condition as, e.g., a Gaussian packet, one would recover the usual physics of electronic billiards. Using the lattice on one hand leads to a discretization of the space, altering the geometric nature of curved edges (see Fig. 1B, D, F); on the other hand, through the stroboscopic nature of the dynamic simulation it allows to “freeze” the system at a very well defined point in its time evolution for the purpose of state detection. The billiard dynamics is characterized by two time scales  $T_L$  and  $T_\lambda$ : The first one is related to the characteristic length of the billiards  $L$  ( $\sim 30$  sites in our simulations), corresponding to the time needed for the first revival of excitations; the second timescale is given by the time needed to perform a swap between two neighboring spins, related to the inter-site coupling strength  $T_\lambda = \pi/(4\lambda)$ . The relation of the two timescales is  $T_L \propto 2LT_\lambda$ . Fig. 1 C-F depict snapshots of the site excitation amplitude after time evolution at two different final times  $t_f$  for billiards R and S: For  $t_f \gtrsim T_L/2$  the effect of different boundary shapes is already visible

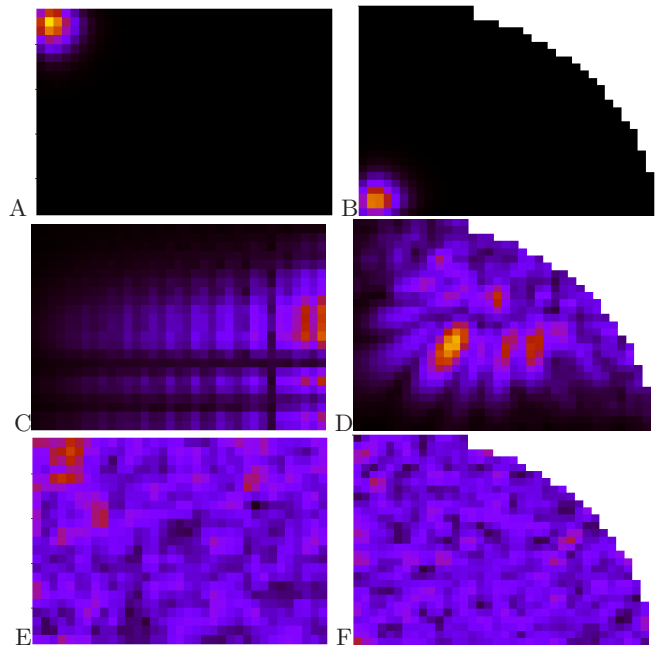


FIG. 1: Snapshots of the populations  $|\psi_t|^2$  time evolution in the rectangular billiard (left) and stadium billiard (right), for  $t = 0^+$  (uppermost figures),  $t \gtrsim T_L/2$  (middle) and  $t = 10 T_L$  (bottom). Color code goes from black (zero) to blue and red with increasing probability.

(Fig. 1 C and D). For longer times,  $t_f \gg T_L$  the collective excitations spread all over the billiards, showing irregular profiles with no distinguishable features at first sight (Fig. 1 E and F). However, for  $t_f \propto n T_L$  ( $n \in \mathbb{N}$ ), a large revival at the initial site is still visible for the rectangular billiard resulting from constructive interference, while this is no longer possible for the stadium billiard. These are the first signatures resembling chaotic and integrable dynamics in billiards realized in optical lattices. In the following we demonstrate that this is indeed the case and that its characteristic features can be detected and quantified experimentally.

We first check the level spacing statistics (LSS) for the two billiards R and S. Following Bohigas' conjecture we expect billiard R to show Poisson LSS, while billiard S should present something different due to the effect of level repulsion. Indeed, as shown in Fig. 2, we find that billiard R displays a well defined Poisson LSS (red squares). For billiard S, instead, we find a Semi-Poisson LSS typical of semi-integrable systems (also appearing in the Anderson Metal-insulator transition) [17]. The complete onset of chaos and the appearance of a Wigner-Dyson distribution is probably prevented due to the significant role still played by periodic orbits. A better convergence to the theoretical distribution can be obtained by considering defects, i.e., empty sites (see below). This allows a better statistics by averaging over  $N_R$  different configurations of defect probabilities

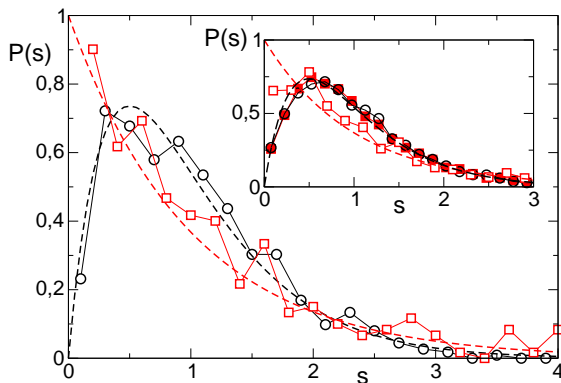


FIG. 2: Level spacing statistic for the billiard R (red squares) and billiard B (black circles). Dotted lines follow the Poisson (red) and Semi-Poisson statistics (black). Inset: LSS averaged over  $N_R = 10$  different configurations of defects with  $P_D = 5 \cdot 10^{-3}$  (empty symbols)  $P_D = 5 \cdot 10^{-2}$  (full symbols). The black [red] dashed line follows the theoretical prediction  $P(s) = 4s \exp(-2s)$  [ $P(s) = \exp(-s)$ ].

( $P_D = 5 \cdot 10^{-2}, 5 \cdot 10^{-3}$ ), as shown in the inset of Fig. 2. Eventually, also billiard R displays Semi-Poisson statistics due to the presence of defects (inset of Fig. 2, red full squares).

The striking differences in the LSS discussed above are reflected in other features of the spin-billiard dynamics that can be measured experimentally, as we show hereafter. We consider in particular the momentum distribution and the fluorescence signal, as used for instance to detect single ions [18]. After its introduction by Peres [19], the survival probability or Fidelity  $F$

$$F = |\langle \psi_{t=0} | \psi_t \rangle|^2, \quad (3)$$

has been very useful to characterize the transition to chaos [20]. Here the main issue, due to the lattice spacing coinciding with optical wavelengths, is single-atom spatial resolution. Therefore, we consider a Coarse Grained Fidelity (CGF) defined as

$$F_n = \left| \left\langle \sum_{\langle i,j \rangle}^{\langle i+n,j+n \rangle} \mathcal{M}(i,j) | \psi_t \right\rangle \right|^2, \quad (4)$$

i.e., the survival probability in a square region around the site  $\{i, j\}$ . The CGF can be obtained via fluorescence measurements in optical lattices without single site addressing, which is at the edge of present day technology [21]. Even if the CGF fails in detecting the finest details of the dynamics it still captures the main differences between the integrable and chaotic systems. In Fig. 3 A and C we show the CGF ( $n = 3$ ) decay in the rectangular (black) and stadium (red) billiards for different disorder settings together with their corresponding auto-correlation functions (Fig. 3 B and D). In spite of the random noise, both the CGF (Fig. 3 C) and its

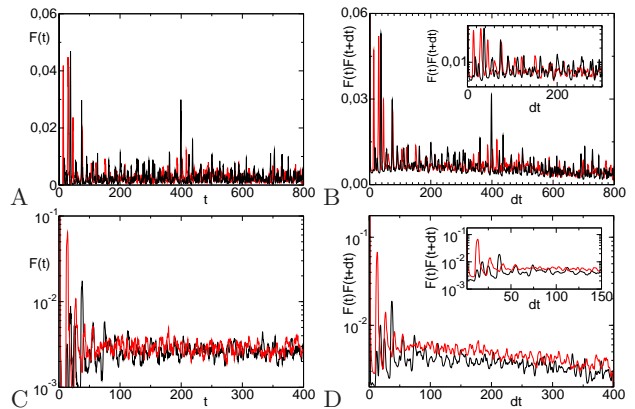


FIG. 3: Coarse grained Fidelity  $F_3$  (A,C) as a function of time for the integrable (black) and chaotic billiard (red) and the auto-correlation of the signals in the left figure (B,D) for  $P_D = \epsilon = 0$  (upper panels) and  $P_D = 5 \cdot 10^{-3}, \epsilon = 10^{-5}, N_R = 10$  (lower panels). Insets: Magnification of the bigger figure.

auto-correlation (Fig. 3 D) reveal the fundamental time scale  $T_L$ . Striking differences appear between R and S billiards: Periodic oscillations persist up to times of the order of  $t_f \gg T_L$  in the integrable case (black), while in the chaotic case (red) a damping shows up on a time scale  $t \gtrsim T_L$  revealing a rapid decay of correlations.

Finally, we investigate the momentum distribution of the magnetization in the two billiards at a final time  $t_f$ : The results are reported in Fig. 4 A and B for the rectangular (left) and stadium billiards (right). Again the results show striking differences: In the integrable case the number of frequencies relevant to the wave function are much less than in the chaotic case. Moreover in the former case there is a structure (even though quite complex) in the spectrum that is absent in the latter one.

*Experimental Implementation* - As mentioned in the introduction spin billiards can be studied experimentally in optical lattices following the idea of the Universal Quantum Simulator [14]. The measurements of the CGF and momentum distribution can be performed via fluorescence and time-of-flight methods respectively [15, 18]. The signatures of chaos we are interested in arise from the evolution of a single-spin excitation corresponding to single-particle signals. In order to attain a sufficient atom number resolution to detect it, an average over different realizations is required. Under ideal conditions, since the evolution is fully deterministic, this should not be a problem and the result would be fully reproducible. However, in a real experiment, errors might introduce differences between repetitions which may result in a corrupted output. The major error sources are two: (i) imperfections in the realization of a square lattice with hundreds of sites with uniform occupation number one, and (ii) side effects

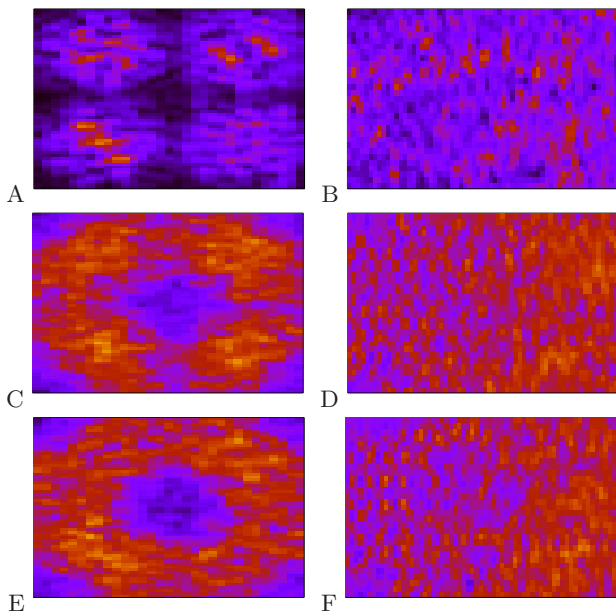


FIG. 4: 2D FT of the Wave function  $F(\omega_x, \omega_y)$  for the rectangular (left) and stadium (right) billiards at time  $t_f = 10 T_L$  for  $P_D = \epsilon = 0$  (A,B);  $P_D = 5 \cdot 10^{-3}, \epsilon = 10^{-5}, N_R = 10$  (C,D); and  $P_D = 10^{-2}, \epsilon = 10^{-5}, N_R = 10$  (E,F). Color code is the same of Fig. 1.

of the parabolic magnetic field trapping the atoms in the studied region of the optical lattice [22]. We can model these errors via the presence of defects or “holes” in the spin billiard (missing atom in a optical lattice site) and errors in the gates performed to simulate the dynamics. The Hamiltonian (1) is then replaced by

$$\mathcal{H}_1 = \lambda \sum_{\langle m, m' \rangle} (\sigma_x^m \sigma_x^{m'} + \sigma_y^m \sigma_y^{m'}) + \sum_m \epsilon(t)(i+j)\sigma_z^m, \quad (5)$$

where  $m = \mathcal{M}_H(i, j)$  takes into accounts the presence of defects and  $\epsilon(t)$  fluctuates in  $[0, \epsilon]$  with flat distribution. We repeat the previous analysis accounting for experimental errors with typical values  $P_D = 5 \cdot 10^{-3}$  and  $\epsilon = 10^{-5}$  averaging over  $N_R$  different configurations [22]. Fig. 3 (lower panels) shows the coarse grained fidelity  $F_3$  and the auto-correlation as a function of time  $R$  and  $S$  billiards in presence of experimental errors. In this case, it is more difficult to distinguish between integrable and chaotic dynamics; however, a careful inspection can still reveal differences. As before, in the integrable case the auto-correlation revivals last for longer times  $t_f \gg T_L$  and their visibility is greater than in the chaotic case. More clear signatures are found again in the momentum distribution (Fig. 4, lower panels): The structures in the frequency domain lasts for very long times in the integrable billiard (even if slightly blurred) while they disappear in the chaotic case.

Finally we would like to highlight the possible developments along the lines presented here: The study and

simulation of weak localization, quantum hall effect, disorder effects, quantum information protocols, entanglement dynamics, and the role of different Hamiltonian and/or parameter regimes. We also point out that a similar analysis could be performed for alternative experimental setups as, e.g., lattices of coupled cavities [23].

We thank M. Greiner and I. Bloch for insightful discussions. This work was supported by the EC grants SCALA and EUROSQIP, by the “Ramón y Cajal” Program of the Spanish Ministry of Education and Science, and by the Excellence Project P07-FQM-3037 of the Andalusian Government.

- 
- [1] see e.g.: Proceedings of the Les Houches Summer School on *Chaos and Quantum Physics*, Les Houches, 1989, M. Giannoni, A. Voros, and J. Zinn-Justin Eds. (North-Holland, Amsterdam, 1991); Proceedings of the International School of Physics “Enrico Fermi” on *Quantum chaos*, Course CXIX, Varenna, 1991, G. Casati, I. Guarneri, and U. Smilansky Eds. (North-Holland, Amsterdam, 1993).
- [2] M.V. Berry and M. Tabor Proc. Roy. Soc. London A **356** 375 (1977); S.W. McDonald and A. N. Kaufman, Phys. Rev. Lett. **42**, 1189 (1979); G. Casati, B.V. Chirikov, and I. Guarneri, *ibid.* **54**, 1350 (1985); R.A. Jalabert, H.U. Baranger and A.D. Stone, *ibid.* **65**, 2442 (1990); G. Casati and T. Prosen, Physica D **131** 293 (1999).
- [3] see e.g.: L. Reichl, *The Transition to Chaos*, Springer-Verlag (2004).
- [4] J. Stein and H-J. Stöckmann, Phys. Rev. Lett. **64**, 2215 (1992).
- [5] H-D. Graf *et al.*, Phys. Rev. Lett. **69**, 1296 (1992).
- [6] N. Davidson *et al.*, Phys. Rev. Lett. **74**, 1311 (1995).
- [7] K. Richter, *Semiclassical Theory of Mesoscopic Quantum Systems* (Springer-Verlag, Berlin, 2000); C.J.Beenakker Rev. Mod. Phys. **69** 731 (1997).
- [8] C.M. Marcus *et al.*, Phys. Rev. Lett. **69**, 506 (1992).
- [9] C.M. Marcus *et al.*, Chaos **3**, 643 (1993); H.U. Baranger, R.A. Jalabert, and A.D. Stone, Chaos **3**, 665 (1993).
- [10] D. M. Zumbühl *et al.*, Phys. Rev. Lett. **89**, 276803 (2002); I. L. Aleiner and V. I. Fal’ko, *ibid.* **87**, 256801 (2001); O. Zeitsev, D. Frustaglia, and K. Richter, *ibid.* **94**, 026809 (2005); *ibid.*, Phys. Rev. B **72**, 155325 (2005).
- [11] C. W. J. Beenakker *et al.*, in “Fundamental Problems of Mesoscopic Physics”, edited by I. V. Lerner, B. L. Altshuler, and Y. Gefen, NATO Science Series II vol. 154 (Kluwer, Dordrecht, 2004); D. Frustaglia, S. Montangero, R. Fazio, Phys. Rev. B **74**, 165326 (2006); J.H. Bardarson and C.W.J. Beenakker, *ibid.* **74**, 235307 (2006); V.A. Gopar and D. Frustaglia, *ibid.* **77**, 153403 (2008).
- [12] F. Miao *et al.*, Science **317**, 1530 (2007).
- [13] M. Lewenstein *et al.*, Adv. Phys. **56**, 243 (2007).
- [14] E. Jané *et al.*, Quantum Inf. and Comp. **3**, 15 (2003); J.J. Garcia-Ripoll, M.A. Martin-Delgado, and J.I.Cirac, Phys. Rev. Lett. **93**, 250405 (2004).
- [15] I. Bloch, J. Dalibard, and W. Zwerger, Rev. Mod. Phys. (in press), arXiv:0704.3011.
- [16] A. Sørensen and K. Mølmer, Phys. Rev. Lett. **83**, 2274 (1999).

- [17] O. Bohigas, in "Chaos and Quantum Physics", Proceedings of the Les Houches Summer School (1989), M. J. Giannoni, A. Voros, and J. Zinn-Justin Eds. (Elsevier, New York, 1991); E. B. Bogomolny, U. Gerland, and C. Schmit, Phys. Rev. E. **59**, R1315, (1999).
- [18] D. Leibfried *et al.*, Rev. Mod. Phys. **75**, 281 (2003).
- [19] A. Peres, Phys. Rev. A **30**, 1610 (1984).
- [20] H.M. Pastawski, P.R. Levstein, and G. Usaj, Phys. Rev. Lett. **75**, 4310 (1995); P. Jacquod, P.G. Silvestrov and C.W.J. Beenakker, Phys. Rev. E **64** 055203 (2001); R. A. Jalabert and H. M. Pastawski, Phys. Rev. Lett. **86**, 2490 (2001); G. Benenti *et al.*, *ibid.* **87**, 227901 (2001); F.M. Cucchietti *et al.*, *ibid.* **91** 210403 (2003).
- [21] A.V. Gorshkov *et al.*, Phys. Rev. Lett. **100**, 093005 (2008).
- [22] M. Greiner, private communication.
- [23] M.J. Hartmann, F.G.S.L. Brandão, and M. B. Plenio, Nat. Phys. **2**, 849 (2006).